Landau-Ginzburg-Devonshire theory of the chiral phase transition in 180° domain walls of $PbTiO_3$

I. Rychetsky [*]
Institute of Physics of the Czech Academy of Sciences, Na Slovance 2, 18200 Prague 8, Czech Republic

W. Schranz and A. Tröster
University of Vienna, Faculty of Physics, Boltzmanngasse 5, 1090 Wien, Austria

(Received 9 April 2023; revised 27 June 2023; accepted 28 August 2023; published 21 September 2023)

A new mechanism leading to a switchable *Bloch*-type polarization in a domain wall separating two ferroelectric domain states is proposed. A biquadratic coupling of the primary order parameter and its gradient originating from inhomogeneous electrostriction triggers the chiral phase transition (*Ising*-to-*Bloch*) in the domain walls (DW) with softening of the local polar mode and anomalous increase of the dielectric susceptibility at the phase transition temperature $T_{DW} < T_c$. This mechanism describes the origin and properties of the polar *Bloch* component, which appears below T_{DW} additionally to the antipolar *Néel* component in the 180° DW of $PbTiO_3$. The tensile strain of the DW plane promotes the development of the *Bloch* polarization.

DOI: 10.1103/PhysRevB.108.104107

I. INTRODUCTION

The tensor properties of domain walls (DWs) in ferroic materials receive increasing interest driven by achievements in technological and measurement methods allowing to fabricate and observe submicron and nanoscale structures. Various methods for modeling of DWs are widely used [1], i.e., first-principle calculations [2], machine-learned force fields [3], phase-field modeling [4], and phenomenological Landau-Ginzburg-Devonshire (LGD) theory [5], which are closely interconnected with the DW symmetry analysis described by layer groups [6–10]. Polarization inside DWs was predicted in some perovskite structures [11,12], where the crucial role was assigned to flexoelectricity [13], rotopolar coupling [8,14], or biquadratic coupling of the primary and secondary order parameters [15].

The possible existence of a polar 180° DW in $PbTiO_3$ (PTO) was reported by several authors. However, the situation is not so clear yet. Based on *ab initio* calculations an *Ising* structure of the DW profile was reported in Ref. [16]. Such a DW would not carry any polarization within the wall. Other authors concluded that the DW contains also a *Néel*-like polarization (asymmetric polarization profile) originating from flexoelectricity [17,18] and a switchable *Bloch* component indicating a ferroelectric phase transition inside the DW [2,19]. The latter behavior was not found to be stable within the LGD approach [17,18], using the common free-energy expansion.

In the present work we show that the symmetry and properties of 180° DW in PTO can be excellently described by extending the LGD potential by a coupling term which originates from inhomogeneous electrostriction.

II. SYMMETRY OF 180° DOMAIN WALLS

PTO exhibits a uniaxial ferroelectric phase transition from cubic to tetragonal structure without multiplication of the unit cell. The symmetry decrease from $Pm\bar{3}m$ to $P4mm$ implies 6 tetragonal domain states (DSs) $1_1 \equiv (-P_s, 0, 0)$, $2_1 \equiv (0, -P_s, 0)$, $3_1 \equiv (0, 0, -P_s)$, and $1_2,\ 2_2,\ 3_2$ with opposite sign of polarization.

To account for the significant interest [16–19], especially in the aforementioned DWs, we consider the 180° DW $(3_1|\mathbf{n}, \mathbf{p}|3_2)$ between the DSs $3_1 \equiv (0, 0, -P_s)$ and $3_2 \equiv (0, 0, P_s)$, with the normal $\mathbf{n} = [1, 0, 0]$ and the microscopic position $\mathbf{p}$ within the unit cell [8,9], implying that the DW profiles depend only on x. The macroscopic tensor properties of DWs described by Landau theory are independent of the microscopic position $\mathbf{p}$ and they are determined by the layer group symmetry of the DW twin $(3_1|\mathbf{n}|3_2)$, which contains 4 elements $T_{12} = \mathbf{T}\{1, m_y, 2_y, \bar{1}\}$, $\mathbf{T}$ are translations parallel with the DW plane [9]. This symmetry implies that the *Néel* component is antisymmetric $P_1(x) = -P_1(-x)$, and it can be nonzero in the whole temperature range below T_c. The *Bloch* component is forbidden by symmetry, since application of m_y yields $P_2(x) = -P_2(x) = 0$. Therefore it could only occur as a result of phase transition lowering the symmetry to $T'_{12} = \mathbf{T}\{1, 2_y\}$. Then the *Bloch* component can be nonzero and must be symmetric: $P_2(x) = P_2(-x) \neq 0$. The polarization profiles and the phase transition in the DW are further analyzed using the Landau-Ginzburg free-energy description.

III. THE FREE ENERGY

The Gibbs free energy can be written as

$$G(\mathbf{P}, \boldsymbol{\sigma}) = G_0 + G_{es} + G_{el} + G_{\text{flex}} + G_{\text{biq}} + G_g, \qquad (1)$$

[*] rychet@fzu.cz

where the individual parts, pure polarization G_0, electrostriction G_{es}, elastic energy G_{el}, gradient term G_g, flexoelectric G_{flex}, biquadratic OP, and its gradient G_{biq} read

$$\begin{aligned} G_0 =& \alpha_1\left(P_1^2+P_2^2+P_3^2\right)+\alpha_{11}\left(P_1^4+P_2^4+P_3^4\right)\\ &+\alpha_{12}\left(P_1^2P_2^2+P_3^2P_2^2+P_1^2P_3^2\right)+\alpha_{123}P_1^2P_2^2P_3^2\\ &+\alpha_{111}\left(P_1^6+P_2^6+P_3^6\right)+\alpha_{112}\left(\left(P_2^4+P_3^4\right)P_1^2\right.\\ &\left.+\left(P_1^4+P_2^4\right)P_3^2+P_2^2\left(P_1^4+P_3^4\right)\right), \end{aligned} \quad (2)$$

$$\begin{aligned} G_{es} =& -\sigma_1\left(P_1^2Q_{11}+P_2^2Q_{12}+P_3^2Q_{12}\right)-\sigma_2\left(P_2^2Q_{11}\right.\\ &\left.+P_1^2Q_{12}+P_3^2Q_{12}\right)-\sigma_3\left(P_3^2Q_{11}+P_1^2Q_{12}+P_2^2Q_{12}\right)\\ &-Q_{44}(P_2P_3\sigma_4+P_1P_3\sigma_5+P_1P_2\sigma_6), \end{aligned} \quad (3)$$

$$\begin{aligned} G_{el} =& -\frac{1}{2}\left(\left(\sigma_1^2+\sigma_2^2+\sigma_3^2\right)s_{11}+2(\sigma_1\sigma_2+\sigma_3\sigma_2+\sigma_1\sigma_3)s_{12}\right.\\ &\left.+\left(\sigma_4^2+\sigma_5^2+\sigma_6^2\right)s_{44}\right), \end{aligned} \quad (4)$$

$$G_g = \frac{1}{2}\left(g_{11}\left(\frac{\partial P_1}{\partial x}\right)^2+g_{44}\left(\frac{\partial P_2}{\partial x}\right)^2+g_{44}\left(\frac{\partial P_3}{\partial x}\right)^2\right), \quad (5)$$

$$\begin{aligned} G_{\text{flex}} =& -\frac{\partial P_1}{\partial x}(f_{11}\sigma_1+f_{12}(\sigma_2+\sigma_3))\\ &-f_{44}\left(\frac{\partial P_2}{\partial x}\sigma_6+\frac{\partial P_3}{\partial x}\sigma_5\right), \end{aligned} \quad (6)$$

$$\begin{aligned} G_{\text{biq}} =& -\sigma_1\left(R_{111}\left(\frac{\partial P_1}{\partial x}\right)^2+R_{121}\left[\left(\frac{\partial P_2}{\partial x}\right)^2+\left(\frac{\partial P_3}{\partial x}\right)^2\right]\right)\\ &-\sigma_2\left(R_{221}\left(\frac{\partial P_2}{\partial x}\right)^2+R_{211}\left(\frac{\partial P_1}{\partial x}\right)^2+R_{231}\left(\frac{\partial P_3}{\partial x}\right)^2\right)\\ &-\sigma_3\left(R_{221}\left(\frac{\partial P_3}{\partial x}\right)^2+R_{211}\left(\frac{\partial P_1}{\partial x}\right)^2+R_{231}\left(\frac{\partial P_2}{\partial x}\right)^2\right)\\ &-R_{441}\left[\sigma_4\left(\frac{\partial P_2}{\partial x}\frac{\partial P_3}{\partial x}\right)\right]-R_{551}\left[\sigma_5\left(\frac{\partial P_1}{\partial x}\frac{\partial P_3}{\partial x}\right)\right.\\ &\left.+\sigma_6\left(\frac{\partial P_1}{\partial x}\frac{\partial P_2}{\partial x}\right)\right]. \end{aligned} \quad (7)$$

G_{flex} and G_{biq} are terms not considered in Ref. [18], the influence of G_{flex} was studied in Ref. [17]. The origin of G_{flex}, G_{es}, and G_{biq} results from the expansion of strain with respect to polarization and its gradients (Appendix A)

$$e_{ij} = f_{ijkl}\frac{\partial P_k}{\partial x_l}+Q_{ijkl}P_kP_l+R_{ijklmn}\frac{\partial P_k}{\partial x_m}\frac{\partial P_l}{\partial x_n},$$

where the terms represent converse flexoelectricity, common electrostriction of the bulk crystal, and gradient electrostriction, respectively. The last term is important at the DW center, where polarization is small but the gradient is big, and it reflects the fact that the DW center is not a high-symmetry structure. The two-suffix notation is used for tensor components, e.g., $R_{231} \equiv R_{223311}$. In cubic symmetry the tensor R_{ijklmn} has 16 nonzero independent components. In G_{flex} and G_{biq}, only the terms that couple strain and polarization are shown. For simplicity we omit the other symmetry-allowed terms that directly couple polarization and its gradients: $\propto P_iP_j\frac{\partial P_k}{\partial x}$ in G_{flex} and $\propto P_iP_j\frac{\partial P_k}{\partial x}\frac{\partial P_l}{\partial x}$ in G_{biq}. The primary effect of these terms is to renormalize coefficients, which for $PbTiO_3$ are not very well known, anyway. However, it should be stressed that independent on the particular choice of the coupling coefficients of the flexoelectric part G_{flex}, the stabilization of a *Bloch* component is not possible at any temperature if the biquadratic gradient coupling part G_{biq} is zero.

Since the DW properties are x dependent, the gradient terms contain only $\partial\Box/\partial x$ derivatives. The quasi-1D DW along the x axis requires mechanical equilibrium $\sigma_1 = \sigma_5 = \sigma_6 = 0$ and compatibility of strains $e_2(x) = e_{2s}$, $e_3(x) = e_{3s}$, $e_4(x) = e_{4s}$, where e_{is} are spontaneous strains of homogeneous domains. Therefore it is convenient to use the thermodynamic potential $F(\mathbf{P}, \sigma_1, \sigma_2, \sigma_6, e_2, e_3, e_4)$ obtained by the Legendre transformation $F = G+\sigma_2e_2+\sigma_3e_3+\sigma_4e_4$. When accounting for zero stress components the flexoelectric and gradient electrostriction parts become

$$G_{\text{flex}} = -f_{12}(\sigma_2+\sigma_3)\frac{\partial P_1}{\partial x}, \quad (8)$$

$$\begin{aligned} G_{\text{biq}} =& -R_{221}\left(\sigma_2\left(\frac{\partial P_2}{\partial x}\right)^2+\sigma_3\left(\frac{\partial P_3}{\partial x}\right)^2\right)\\ &-R_{211}\left(\sigma_2\left(\frac{\partial P_1}{\partial x}\right)^2+\sigma_3\left(\frac{\partial P_1}{\partial x}\right)^2\right)\\ &-R_{231}\left(\sigma_2\left(\frac{\partial P_3}{\partial x}\right)^2+\sigma_3\left(\frac{\partial P_2}{\partial x}\right)^2\right)\\ &-R_{441}\left[\sigma_4\left(\frac{\partial P_2}{\partial x}\frac{\partial P_3}{\partial x}\right)\right]. \end{aligned} \quad (9)$$

For the sake of simplicity we further keep only the R_{231} term, and neglect all remaining ones (i.e., $R_{221} = R_{211} = R_{441} = 0$), since some of them only renormalize the gradient coefficients; P_1 is already accounted for in G_{flex}, and shear is expected to be zero. Taking into account all above the potential, F is expressed as

$$F = F_0+F_{\text{flex}}+F_{\text{biq}}, \quad (10)$$

where

$$\begin{aligned} F_0 =& b_1P_1^2+b_2P_2^2+b_3P_3^2+b_{11}P_1^4+b_{22}\left(P_2^4+P_3^4\right)\\ &+b_{12}\left(P_1^2P_2^2+P_1^2P_3^2\right)+b_{23}P_2^2P_3^2\\ &+\alpha_{123}P_1^2P_2^2P_3^2+\alpha_{111}\left(P_1^6+P_2^6+P_3^6\right)\\ &+\alpha_{112}\left(\left(P_2^4+P_3^4\right)P_1^2+\left(P_1^4+P_2^4\right)P_3^2+P_2^2\left(P_1^4+P_3^4\right)\right)\\ &+\frac{1}{2}\left(g_{11}\left(\frac{\partial P_1}{\partial x}\right)^2+g_{44}\left(\frac{\partial P_2}{\partial x}\right)^2+g_{44}\left(\frac{\partial P_3}{\partial x}\right)^2\right), \end{aligned} \quad (11)$$

$$F_{\text{flex}} = f'_{12}\frac{\partial P_1}{\partial x}\left(P_2^2+P_3^2\right), \quad (12)$$

$$F_{\text{biq}} = r_{23}\left[P_2^2\left(\frac{\partial P_3}{\partial x}\right)^2+P_3^2\left(\frac{\partial P_2}{\partial x}\right)^2\right], \quad (13)$$

TABLE I. Free energy parameters [18,20,21].

α_1	$3.8(T-752\mathrm{K})\times 10^5\,\mathrm{C^{-2}m^2N}$	Q_{11}	$0.089\,\mathrm{C^{-2}m^4}$	g_{11}	$2.0\times 10^{-10}\,\mathrm{m^4C^{-2}N}$
α_{11}	$-0.73\times 10^8\,\mathrm{C^{-4}m^6N}$	Q_{12}	$-0.026\,\mathrm{C^{-2}m^4}$	g_{44}	$1.0\times 10^{-10}\,\mathrm{m^4C^{-2}N}$
α_{12}	$7.5\times 10^8\,\mathrm{C^{-4}m^6N}$	Q_{44}	$0.0337\,\mathrm{C^{-2}m^4}$		
α_{111}	$2.6\times 10^8\,\mathrm{C^{-6}m^{10}N}$	s_{11}	$8.0\times 10^{-12}\,\mathrm{m^2N^{-1}}$		
α_{112}	$6.1\times 10^8\,\mathrm{C^{-6}m^{10}N}$	s_{12}	$-2.5\times 10^{-12}\,\mathrm{m^2N^{-1}}$		
α_{123}	$-37\times 10^8\,\mathrm{C^{-6}m^{10}N}$	s_{44}	$9.0\times 10^{-12}\,\mathrm{m^2N^{-1}}$		

where $f'_{12}=f_{12}F$, $r_{23}=R_{231}A$ $(A>0)$, and b coefficients are explicitly written in Appendix B. The numerical values of the coefficients for PTO are shown in Tables I and II. The spontaneous polarization is $P_s=\sqrt{\frac{-a_{11}+\sqrt{a_{11}^2-3a_1a_{111}}}{3a_{111}}}$. It is reasonable to assume that the gradient-electrostriction coefficient R_{231} has the same sign as the electrostriction coefficient Q_{12}, since off-diagonal tensor components are often negative, i. e., $R_{231}<0$, which implies $r_{23}<0$. In such case a stability condition is also required: $r_{23}P_s^2+g_{44}/2>0$. F_0 was already discussed in Ref. [18]. It is shown below that F_0 alone does not lead to the DW polarization, while the flexoelectric coupling induces the *Néel* component P_1, and the biquadratic coupling r_{23} of the OP and its gradient can cause the appearance of the *Bloch* component P_2 below T_{DW}, depending on its value. For brevity, scaled numerical values of f'_{12} and r_{23} are further used, i.e., their units are $[f'_{12}]=10^{-1}\,\mathrm{m^5C^{-3}N}$ and $[r_{23}]=10^{-10}\,\mathrm{m^8C^{-4}N}$. Let us stress that the values of f'_{12} and r_{23} are not known and we treat them as free parameters in the free energy F, Eq. (10).

IV. 180° DOMAIN WALLS

The polarization profile can be obtained by minimizing the free energy functional $\mathcal{L}=\int_{-\infty}^{\infty}F(\mathbf{P}(x),\partial_x\mathbf{P}(x))dx$ with proper boundary conditions $P_1(\pm\infty)=0$, $P_2(\pm\infty)=0$, $P_3(\pm\infty)=\pm P_s$, see Sec. II. In practice, this can be achieved by direct minimization of the discretized (finite-difference) free energy. An example of the DW profile at low temperatures and with specifically chosen values of f'_{12} and r_{23} is shown in Fig. 1. Alternatively, it can be obtained by solving Lagrange-Euler (LE) equations. Let us first assume $F=F_0$, i. e., $f'_{12}=r_{23}=0$. Then the LE equations can be solved explicitly and the *Ising* DW profile is obtained:

$$P_1=P_2=0,\;\;P_3=\frac{P_s\tanh(x/2L)}{\sqrt{\eta/\cosh^2(x/2L)+1}},\tag{14}$$

$\eta=\frac{b_3+2b_{33}P_s^2}{2b_3+b_{33}P_s^2}$, $L=\sqrt{\frac{g_{44}}{30a_{111}P_s^4+2b_3+12b_{33}P_s^2}}$. In Ref. [18] the reduced free energy F_0 was considered and the possibility of nonzero P_1 and P_2 was mentioned. But it will be shown that in PTO below $T_c=765$ K the *Ising* profile is in fact always stable when calculated from F_0. In order to get nonzero polarization at the DW center additional free energy terms are needed. At first, only the flexoelectric term F_{flex} is considered: $f'_{12}\neq 0$, $r_{23}=0$. It leads to a nonzero antisymmetric *Néel* component $P_1\propto\frac{\partial P_3^2}{\partial x}$ (and $P_2=0$) in the whole temperature range below T_c and it is in accord with the DW symmetry in Sec. II: $P_1(-x)=-P_1(x)$. The typical antisymmetric *Néel* DW profile is obtained from Fig. 1 by setting $P_2=0$. For $f'_{12}<0$ it possesses head-to-head configuration (see Fig. 1), while for $f'_{12}>0$ it has tail-to-tail configuration, which corresponds to P_1 in Fig. 1 taken with negative sign. For simplicity's sake we do not encounter depolarizing fields here.

The *Bloch* component P_2 can occur by introducing a biquadratic term of the OP and its gradient. Let us first assume a zero flexoelectric term $f'_{12}=0$, $r_{23}\neq 0$. The typical *Bloch* profile is obtained by setting $P_1=0$ in Fig. 1. The discussion of symmetry in Sec. II indicates that a nonzero P_2 could appear only due to a phase transition at T_{DW} accompanied by a decrease of the DW symmetry. Stability of the *Ising* solution Eq. (14), with respect to a small disturbance $P_2=0+\delta_2$, is inspected by solving the eigenvalue problem (equation of motion of δ_2) [15], see Appendix C:

$$\begin{aligned}\Gamma^{-1}\omega_0^2\delta_2=&-2\delta_2\big(a_{112}P_3^4+b_2+b_{23}P_3^2+r_{23}P_{3,x}^2\big)\\&+\delta_{2,xx}\big(2r_{23}P_3^2+g_{44}\big)+4r_{23}P_3P_{3,x}\delta_{2,x}.\end{aligned}\tag{15}$$

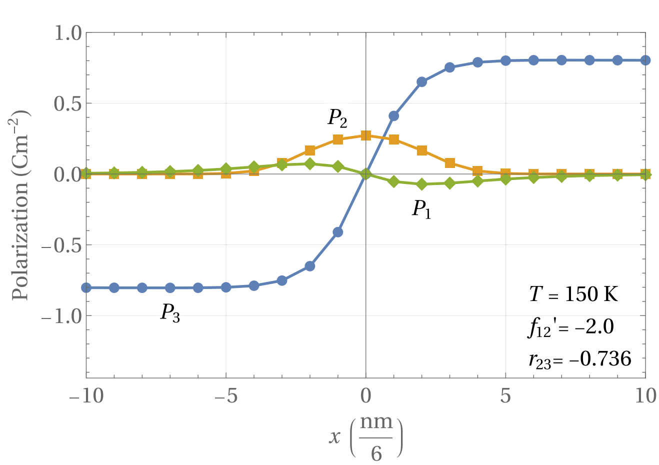

FIG. 1. The most general profile, mixed *Bloch*+*Néel*, at low temperatures $P_1\neq 0$, $P_2\neq 0$. Generally, in the *Bloch* profile $P_1=0$, $P_2\neq 0$; in the *Néel* profile $P_1\neq 0$, $P_2=0$; and in the *Ising* profile $P_1=0$, $P_2=0$. The units of f'_{12} and r_{23} are $[f'_{12}]=10^{-1}\,\mathrm{m^5C^{-3}N}$ and $[r_{23}]=10^{-10}\,\mathrm{m^8C^{-4}N}$.

TABLE II. Auxiliary parameters.

$A=\frac{Q_{11}s_{11}-Q_{12}s_{12}}{s_{11}^2-s_{12}^2}$	$1.12\times 10^{10}\,\mathrm{C^{-2}m^2N}$
$B=\frac{Q_{12}s_{11}-Q_{11}s_{12}}{s_{11}^2-s_{12}^2}$	$2.51\times 10^{8}\,\mathrm{C^{-2}m^2N}$
$C=\frac{s11}{2(s11^2-s12^2)}$	$6.93\times 10^{10}\,\mathrm{m^{-2}N}$
$D=\frac{-s12}{s11^2-s12^2}$	$4.33\times 10^{10}\,\mathrm{m^{-2}N}$
$E=\frac{-Q_{12}}{s11+s12}$	$4.73\times 10^{9}\,\mathrm{C^{-2}m^2N}$
$F=\frac{Q_{11}+Q_{12}}{s11+s12}$	$1.15\times 10^{10}\,\mathrm{C^{-2}m^2N}$

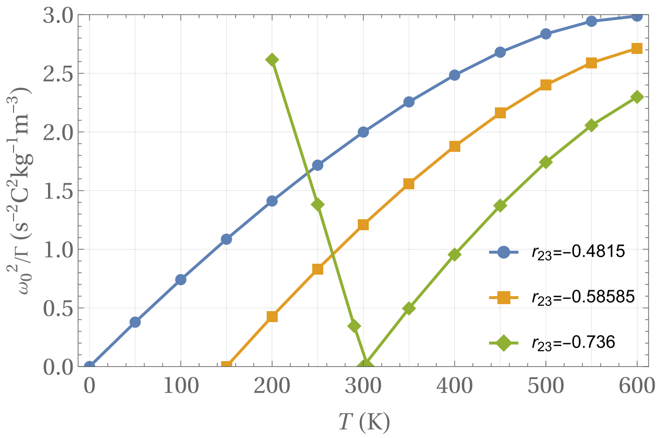

FIG. 2. The temperature dependence of the DW soft mode for different values of r_{23}. The phase transition occurs at temperatures $T_{DW} = 0,\ 150,\ 305$ K. The increase of ω_0^2 below $T_{DW} = 305$ K is also shown.

The instability of the mode δ_2 occurs when $\omega_0^2 < 0$. For positive ω_0^2 the contribution of δ_2 to the susceptibility reads $\Delta\chi = \Gamma/\varepsilon_0\omega_0^2$. $\Delta\chi$ is defined as $\Delta\chi = \delta_{2,A}/E$, where $\delta_{2,A}$ is an amplitude of the polar $\delta_2(x)$ mode and E is an electric field, see Appendix C. The analytic solution of the differential equation [Eq. (15)] is unknown and we solved it numerically for several values of the biquadratic (of the OP and its gradient) coefficient r_{23}, Fig. 2. It turns out that the phase transition in the DW occurs at $T_{DW} > 0$ if $r_{23} < -0.4815$. The effect of negative r_{23} can be seen from the quadratic P_2^2 term at the DW center $(b_2 + r_{23}P_{3,x}^2)P_2^2$, which decreases if $r_{23} < 0$. Near above T_{DW}, $\omega_0^2 \propto (T - T_{DW})$ (see Fig. 2). Below T_{DW} the symmetric *Bloch* component $P_2(x)$ appears, its shape is shown in Fig. 1. Below T_{DW}, ω_0^2 of the polar mode was calculated by solving the coupled equations of motion of δ_2 and δ_3 obtained from Eq. (C4). It exhibits a typical hardening $\omega_0^2 \propto (T_{DW} - T)$ shown in Fig. 2. The corresponding dielectric susceptibility $\Delta\chi$ around the phase transition at $T_{DW} = 305$ K exhibits a $1/|T - T_{DW}|$ divergence, Fig. 3, characteristic of a ferroelectric phase transition. The temperature dependence of the amplitude of the $P_2(x)$ profile is $P_{2,A} \approx (T_{DW} - T)^{1/2}$, see the solid line in Fig. 4. A similar softening of the P_2 polar mode, its freeze-out below T_{DW}, and divergent susceptibility was obtained by Monte Carlo (MC) simulations in Ref. [19].

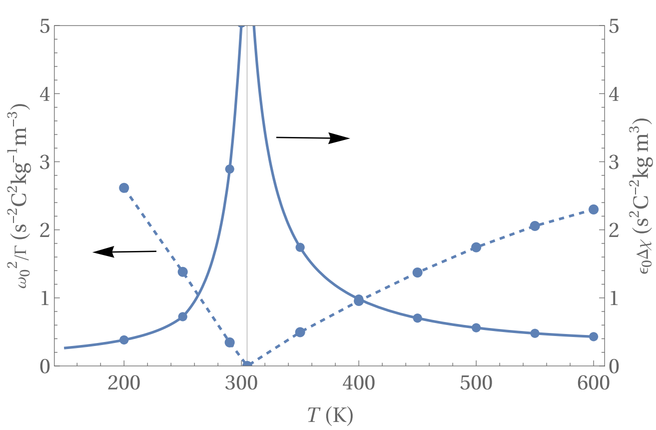

FIG. 3. The susceptibility divergence $\propto 1/|T - T_{DW}|$ at $T_{DW} = 305$ K ($r_{23} = -0.736$). The softening of ω_0^2, the same as in Fig. 2, is also shown for reference.

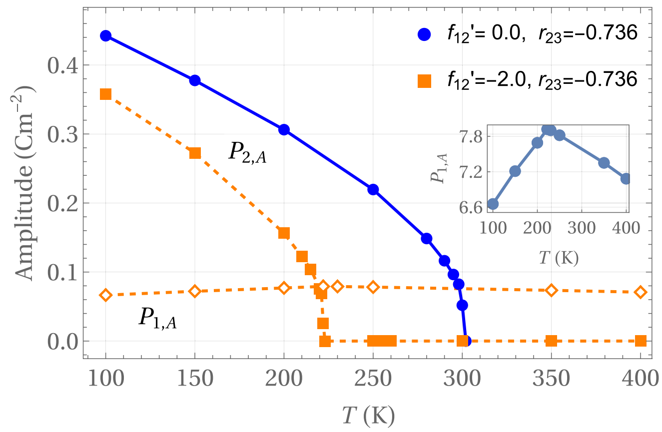

FIG. 4. Temperature dependence of the *Bloch* component $P_{2,A}$ and *Néel* component $P_{1,A}$ for 2 values of f_{12}'. Full line shows the *Ising*→*Bloch* transition at $T_{DW} \approx 305$ K, $P_{1,A} = 0$. Dashed lines show the transition *Néel*→*Bloch*+*Néel* at lower $T_{DW} \approx 220$ K, $P_{1,A} \neq 0$ at all temperatures. The inset shows a tiny cusp of $P_{1,A}$ at $T_{DW} \approx 220$ K, indicating the competition between the *Néel* and *Bloch* components.

The interrelation between the *Néel* and *Bloch* components comes into play when concurrently $f_{12}' \neq 0$ and $r_{23} \neq 0$. The component P_1 exists in the whole temperature range and T_{DW} is shifted to lower temperatures, see the dashed lines in Fig. 4. Below T_{DW} the P_1 and P_2 components coexist (mixed *Néel-Bloch* profile). The inset in Fig. 4 shows that P_1 exhibits a tiny cusp at T_{DW}, reflecting the competition between P_1 and P_2. The polar mode softening and the anomalous susceptibility are similar, as shown in Fig. 3 for the previous case.

The inhomogenous electrostriction results in an increase of stress components σ_2 and σ_3 at the DW center, Fig. 5. The dashed lines correspond to the DW profile Eq. (14) without biquadratic gradient coupling. The substantial increase of the

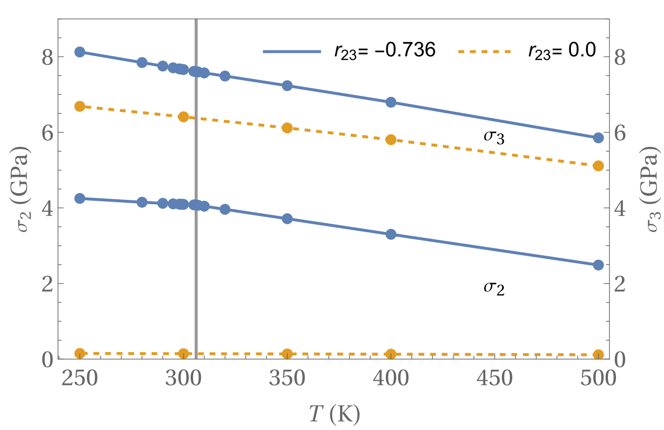

FIG. 5. Temperature dependence of inhomogeneous stress components in the DW center, with biquadratic term (solid lines) and without biquadratic term (dashed lines). Flexoelectric coupling is set to zero.

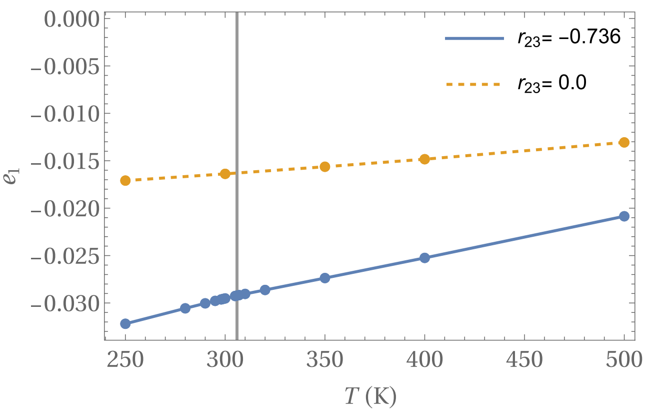

FIG. 6. Temperature dependence of inhomogeneous strain in the DW center, with (solid lines) and without (dashed lines) biquadratic term. Flexoelectric coupling is set to zero.

tensile stress σ_2 along the y axis after including the biquadratic gradient coupling supports the appearance of the P_2 polarization and the corresponding symmetry reduction. As a result, the DW center is compressed along the x direction, Fig. 6.

V. SUMMARY

The layer group symmetry of a 180° DW in $PbTiO_3$ indicates the existence of an unswitchable antisymmetric *Néel* P_1 polarization around the DW center in the whole temperature range below T_c and within the Landau-Ginzburg description it is shown to be induced by the flexoelectric term. Similar results concerning the flexoelectric term were also obtained by phase-field modeling [17]. In general, based on symmetry considerations, it is clear that the *Néel* component is present in every DW. Here, we have shown that the symmetric switchable *Bloch* polarization P_2 occurs due to a phase transition in the domain wall at $T_{DW} < T_c$, which is driven by the biquadratic coupling of the OP and its gradient. This new term can be understood resulting from inhomogeneous electrostriction, which in contrast to bulk electrostriction becomes effective in the center of the 180° DW of PTO. The softening of the polar mode, divergent susceptibility, and the temperature dependence of P_2 below T_{DW} are in excellent agreement with the results from first-principles calculations [2,19].

ACKNOWLEDGMENTS

This work was supported by Operational Program Research, Development, and Education (financed by European Structural and Investment Funds and by the Czech Ministry of Education, Youth, and Sports), Project No. SOLID21-CZ.02.1.01/0.0/0.0/16_019/0000760).

APPENDIX A: STRAIN EXPANSION

Expansion of strain with respect to P_i and $\partial P_j/\partial x_k$ up to second order reads

$$e_{ij} = d_{ijk}P_k + f_{ijkl}\frac{\partial P_k}{\partial x_l} + Q_{ijkl}P_kP_l + T_{ijklm}P_k\frac{\partial P_l}{\partial x_m} + R_{ijklmn}\frac{\partial P_k}{\partial x_m}\frac{\partial P_l}{\partial x_n}, \tag{A1}$$

where the terms are piezoelectricity, flexoelectricity, bulk electrostriction, a rank-5 tensor property, and "gradient electrostriction," respectively. For cubic symmetry $Pm\bar{3}m$ rank 3 and 5 tensors are zero, $d_{ijk} = T_{ijklm} = 0$. Bulk electrostriction contributes in the bulk sample, while it is zero in DWs, where polarization is zero. On the contrary, gradient electrostriction is nonzero inside DWs and zero in the bulk.

APPENDIX B: COEFFICIENTS

The $'b'$ coefficients in F_0 Eq. (11):

$$\begin{aligned}
b_1 &= a_1 - \frac{P_s^2 Q_{12}(Q_{11}+Q_{12})}{s_{11}+s_{12}},\\
b_2 &= a_1 + \frac{P_s^2\left(s_{12}\left(Q_{11}^2+Q_{12}^2\right) - 2Q_{11}Q_{12}s_{11}\right)}{s_{11}^2 - s_{12}^2},\\
b_3 &= a_1 - \frac{P_s^2\left(s_{11}\left(Q_{11}^2+Q_{12}^2\right) - 2Q_{11}Q_{12}s_{12}\right)}{s_{11}^2 - s_{12}^2},\\
b_{11} &= a_{11} + \frac{Q_{12}^2}{s_{11}+s_{12}},\\
b_{12} &= a_{12} + \frac{Q_{12}(Q_{11}+Q_{12})}{s_{11}+s_{12}},\\
b_{22} &= a_{11} + \frac{s_{11}\left(Q_{11}^2+Q_{12}^2\right) - 2Q_{11}Q_{12}s_{12}}{2s_{11}^2 - 2s_{12}^2},\\
b_{23} &= a_{12} - \frac{s_{12}\left(Q_{11}^2+Q_{12}^2\right) - 2Q_{11}Q_{12}s_{11}}{s_{11}^2 - s_{12}^2} + \frac{Q_{44}^2}{2s_{44}}.
\end{aligned} \tag{B1}$$

The reduced gradient electrostriction Eq. (13) and flexoelectric Eq. (12) parts:

$$\begin{aligned}
F_{\mathrm{biq}} + F_{\mathrm{flex}} = &\\
&- R_{231}\left\{-A\left(\left(\frac{\partial P_3}{\partial x}\right)^2 P_2^2 + \left(\frac{\partial P_2}{\partial x}\right)^2 P_3^2\right)\right.\\
&+ E\left(\left(\frac{\partial P_3}{\partial x}\right)^2 + \left(\frac{\partial P_2}{\partial x}\right)^2\right)P_1^2\\
&+ A\left(\frac{\partial P_2}{\partial x}\right)^2 {P_s}^2 + B\left(\frac{\partial P_3}{\partial x}\right)^2 {P_s}^2\\
&\left.- B\left(\left(\frac{\partial P_2}{\partial x}\right)^2 P_2^2 + \left(\frac{\partial P_3}{\partial x}\right)^2 P_3^2\right)\right\}\\
&+ R_{231}^2\left\{\left(\left(\frac{\partial P_2}{\partial x}\right)^4 + \left(\frac{\partial P_3}{\partial x}\right)^4\right)C\right.\\
&\left.+ \left(\frac{\partial P_2}{\partial x}\right)^2\left(\frac{\partial P_3}{\partial x}\right)^2 D\right\}\\
&+ f_{12}F\left(\frac{\partial P_1}{\partial x}\right)\left(P_2^2 + P_3^2\right) + \frac{f_{12}^2}{s_{11}+s_{12}}\left(\frac{\partial P_1}{\partial x}\right)^2\\
&+ \frac{R_{231}f_{12}}{s_{11}+s_{12}}\left(\left(\frac{\partial P_3}{\partial x}\right)^2 + \left(\frac{\partial P_2}{\partial x}\right)^2\right)\left(\frac{\partial P_1}{\partial x}\right)
\end{aligned}$$

$$\approx R_{231}A\left(\left(\frac{\partial P_3}{\partial x}\right)^2 P_2^2 + \left(\frac{\partial P_2}{\partial x}\right)^2 P_3^2\right)$$
$$+ f_{12}F\left(\frac{\partial P_1}{\partial x}\right)(P_2^2 + P_3^2), \tag{B2}$$

where we keep only two terms. The auxiliary coefficients A to F are positive, see Table II. All other terms are neglected—we neglect higher than second-order gradients $B << A$, terms renormalizing gradients, P_1 is kept only in the flexoelectric part.

APPENDIX C: VARIATION

$$\mathcal{L} = \int_{-\infty}^{\infty} F(\mathbf{P}(x), \partial_x \mathbf{P}(x))dx, \tag{C1}$$

$$\delta\mathcal{L} = \int_{-\infty}^{\infty} \frac{\delta\mathcal{L}}{\delta\mathbf{P}}\delta\mathbf{P}dx = \int_{-\infty}^{\infty}\left(\frac{\partial L}{\partial\mathbf{P}} - \frac{d}{dx}\frac{\partial L}{\partial\dot{\mathbf{P}}}\right)\delta\mathbf{P}dx. \tag{C2}$$

The DW profiles $\boldsymbol{\mathcal{P}}$ are solutions of three equilibrium equations

$$\frac{\delta\mathcal{L}}{\delta P_i} \equiv \left(\frac{\partial L}{\partial P_i} - \frac{d}{dx}\frac{\partial L}{\partial\dot{P}_i}\right) = 0,\ \ i = 1, 2, 3. \tag{C3}$$

A small perturbation $\mathbf{P} = \boldsymbol{\mathcal{P}} + \boldsymbol{\delta}$ leads to three equations of motion

$$\Gamma^{-1}\ddot{\delta}_i = -\Gamma^{-1}\omega_0^2\delta_i = -\left.\frac{\delta\mathcal{L}}{\delta P_i}\right|_{\mathbf{P}\to\boldsymbol{\mathcal{P}}+\boldsymbol{\delta}}, \tag{C4}$$

where on the right-hand side only the linear terms in $\boldsymbol{\delta}$ are kept. The perturbation is assumed as $\boldsymbol{\delta} \propto e^{i\omega x}$, the coefficient $\Gamma = ne^2/m$, where m, e, n are mass, charge, and density of ions, respectively, $[\Gamma] = \mathrm{kg}^{-1}\mathrm{m}^{-3}\mathrm{C}^2$. The DW profile becomes unstable when the smallest eigenvalue $\omega_0^2 < 0$. The static susceptibility of the polar eigenmode $\delta_2(x)$ is defined as $\Delta\chi \equiv \delta_{2,A}/E = \Gamma/\varepsilon_0\omega_0^2$, where $\delta_{2,A}$ is an amplitude of the polar mode. In case of the *Ising* profile the three equations in Eq. (C4) are decoupled.

[1] D. Meier, J. Seidel, M. Gregg, and R. Ramesh, *Domain Walls: From Fundamental Properties to Nanotechnology Concepts* (Oxford University Press, Oxford, 2020).

[2] J. Íñiguez, First-principles studies of structural domain walls, in *Domain Walls: From Fundamental Properties to Nanotechnology Concepts* (Oxford University Press, Oxford, 2020).

[3] A. Tröster, C. Verdi, C. Dellago, I. Rychetsky, G. Kresse, and W. Schranz, Hard antiphase domain boundaries in strontium titanate unravelled using machine-learned force fields, Phys. Rev. Mater. **6**, 094408 (2022).

[4] B. Völker, P. Marton, C. Elsässer, and M. Kamlah, Multiscale modeling for ferroelectric materials: A transition from the atomic level to phase-field modeling, Continuum Mech. Thermodyn. **23**, 435 (2011).

[5] P. Marton, I. Rychetsky, and J. Hlinka, Domain walls of ferroelectric $BaTiO_3$ within the Ginzburg-Landau-Devonshire phenomenological model, Phys. Rev. B **81**, 144125 (2010).

[6] W. Schranz, I. Rychetsky, and J. Hlinka, Polarity of domain boundaries in nonpolar materials derived from order parameter and layer group symmetry, Phys. Rev. B **100**, 184105 (2019).

[7] W. Schranz, A. Tröster, and I. Rychetsky, Contributions to polarization and polarization switching in antiphase boundaries of $SrTiO_3$ and $PbZrO_3$, J. Appl. Phys. **128**, 194101 (2020).

[8] W. Schranz, C. Schuster, A. Tröster, and I. Rychetsky, Polarization of domain boundaries in $SrTiO_3$ studied by layer group and order-parameter symmetry, Phys. Rev. B **102**, 184101 (2020).

[9] I. Rychetsky, W. Schranz, and A. Tröster, Symmetry and polarity of antiphase boundaries in $PbZrO_3$, Phys. Rev. B **104**, 224107 (2021).

[10] W. Schranz, A. Tröster, and I. Rychetsky, Signatures of polarity in ferroelastic domain walls and antiphase boundaries of $SrTiO_3$ and other perovskites, J. Alloys Compd. **890**, 161775 (2022).

[11] V. Stepkova, P. Marton, and J. Hlinka, Stress-induced phase transition in ferroelectric domain walls of $BaTiO_3$, J. Phys.: Condens. Matter **24**, 212201 (2012).

[12] P. Marton, V. Stepkova, and J. Hlinka, Divergence of dielectric permittivity near phase transition within ferroelectric domain boundaries, Phase Transitions **86**, 103 (2013).

[13] E. A. Eliseev, S. V. Kalinin, Y. Gu, M. D. Glinchuk, V. Khist, A. Borisevich, V. Gopalan, L.-Q. Chen, and A. N. Morozovska, Universal emergence of spatially modulated structures induced by flexoantiferrodistortive coupling in multiferroics, Phys. Rev. B **88**, 224105 (2013).

[14] A. Schiaffino and M. Stengel, Macroscopic Polarization from Antiferrodistortive Cycloids in Ferroelastic $SrTiO_3$, Phys. Rev. Lett. **119**, 137601 (2017).

[15] A. K. Tagantsev, E. Courtens, and L. Arzel, Prediction of a low-temperature ferroelectric instability in antiphase domain boundaries of strontium titanate, Phys. Rev. B **64**, 224107 (2001).

[16] B. Meyer and D. Vanderbilt, *Ab initio* study of ferroelectric domain walls in $PbTiO_3$, Phys. Rev. B **65**, 104111 (2002).

[17] Y.-J. Wang, J. Li, Y.-L. Zhu, and X.-L. Ma, Phase-field modeling and electronic structural analysis of flexoelectric effect at 180° domain walls in ferroelectric $PbTiO_3$, J. Appl. Phys. **122**, 224101 (2017).

[18] R. K. Behera, C.-W. Lee, D. Lee, A. N. Morozovska, S. B. Sinnott, A. Asthagiri, V. Gopalan, and S. R. Phillpot, Structure and energetics of 180° domain walls in $PbTiO_3$ by density functional theory, J. Phys.: Condens. Matter **23**, 175902 (2011).

[19] J. C. Wojdeł and J. Íñiguez, Ferroelectric Transitions at Ferroelectric Domain Walls Found from First Principles, Phys. Rev. Lett. **112**, 247603 (2014).

[20] M. J. Haun, E. Furman, S. J. Jang, H. A. McKinstry, and L. E. Cross, Thermodynamic theory of $PbTiO_3$, J. Appl. Phys. **62**, 3331 (1987).

[21] Y. Li, S. Hu, Z. Liu, and L. Chen, Effect of substrate constraint on the stability and evolution of ferroelectric domain structures in thin films, Acta Mater. **50**, 395 (2002).